Using the DRESP3 to improve multidisciplinary optimization

Gregory J. Michels[*], Victor L. Genberg
Sigmadyne, Inc.
803 West Avenue, Rochester, NY 14611

By linking predictive methods from multiple engineering disciplines, engineers are able to compute more meaningful predictions of a product's performance. By coupling mechanical and optical predictive techniques mechanical design can be performed to optimize optical performance. This paper demonstrates how the DRESP3 feature in MD Nastran's SOL 200 can be used to perform mechanical design optimization on a high precision adaptive optical imaging system. While mechanical design parameters are treated as the design variables, the weight of the primary mirror is minimized while the adaptively corrected optical imaging performance is constrained to a requirement.

Keywords: Optimization, DRESP3, Multidisciplinary, Design, Aerospace, MD Nastran, Optic

1   INTRODUCTION

Multidisciplinary optimization has been the focus of much recent work.[1-20] By linking predictive methods from multiple engineering disciplines, engineers are able to compute more meaningful predictions of a product's performance and improve the efficiency of the design process. In the design of precision optical systems, such as those used for imaging and communication, the optical performance is directly affected by the mechanical behavior of the system. Dynamic disturbances, thermoelastic deformation, and other operational loads cause the precisely formed optical surfaces of an optical system to move and deform. Even deformations on the nanometer level can have a profound impact on how well some optical systems perform. By coupling mechanical and optical predictive techniques mechanical design can be performed to optimize optical performance.
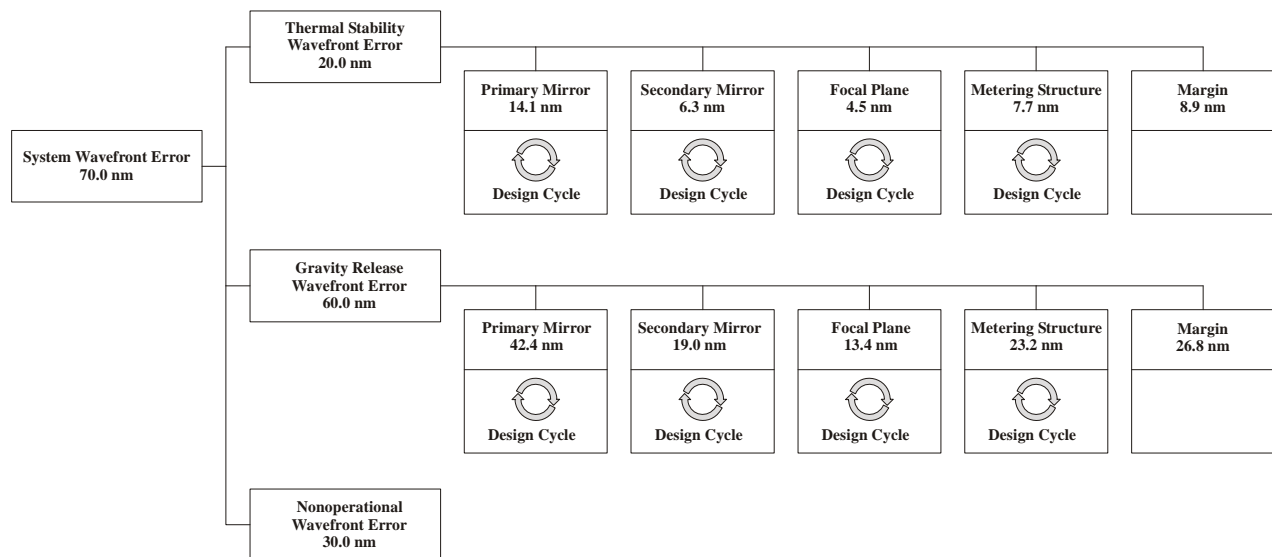

Figure 1: Example wavefront requirement budget for an optical system.

A common technique in the development of an optical system is to develop the mechanical design of individual subsystems by independent parallel processes. These designs are developed to requirements which have been flowed down from a top

---

[*] Correspondence: Email: michels@sigmadyne.com; www: http://www.sigmadyne.com; Telephone: (585) 235-6892

level system requirement as shown in Figure 1. This flow down of requirements to the various subsystems is done by experience and with much iteration as design teams negotiate for rebalancing of the allocations. This is done because prediction of an optical system's performance requires the use of optical design software with imported mechanical analysis results. Since such optical design tools are not integrated within any finite element tools in a widely available fashion for use in automatic design optimization, performing design trades on system level performance is cumbersome. While attempts have been made to integrate optical design software with mechanical finite element tools, there has been no widely available tool with which mechanical engineers can compute system level optical performance metrics within mechanical analysis software for a wide array of problems. [11,16,18]

This paper demonstrates how the DRESP3 feature can be used to predict the system wavefront error of a high precision adaptive optical imaging system to support design optimization in MD Nastran's SOL 200. While the weight of the primary mirror is minimized and mechanical design parameters are treated as the design variables, the adaptively corrected optical imaging performance of an orbiting telescope is held to a requirement.

2   ADAPTIVE OPTICS SIMULATION

It is of particular interest to be able to compute the corrected performance of an adaptive optical system. Since the ability of adaptive optical surfaces to deform into any desired shape is limited by their mechanical characteristics (e.g., stiffness and actuator layout), such predictive capability is required in designing the optical system to maximize the system's corrected performance. We introduce the methods of adaptive optics simulation in the following two subsections. The first deals with adaptive control of a single surface while the second deals with adaptive control of an entire optical system of multiple surfaces.

2.1   Single Surface Performance

Adaptive simulation of a single surface can be represented by the pictorial equation in Figure 2.[14] The first term on the left-hand side represents an input disturbance to the optical system which may be an aberrated incident wavefront or a deformation of the adaptive surface due to environmental loading. The other terms on the left hand side are called actuator influence functions and each represent the shape of the optical surface due to an arbitrary input of a single actuator. The term on the right hand side is the resulting surface due to the effect of the initial disturbance plus the effect of the actuators. The goal of adaptive simulation is to find the actuator control inputs x_1, x_2,…,x_n which minimizes the surface deformation on the right hand side.

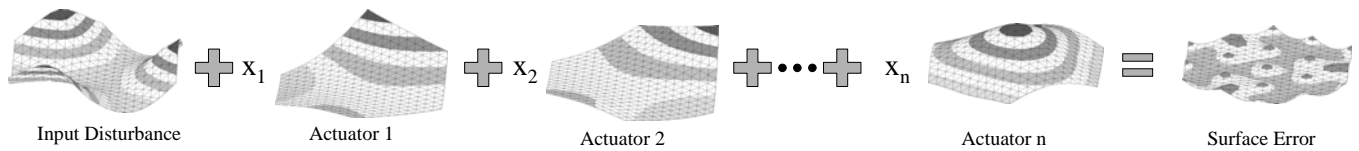| Input Disturbance | Actuator 1 | Actuator 2 | Actuator n | Surface Error |

Figure 2: Pictorial equation of single surface adaptive simulation.

Mathematically, adaptive simulation of a single surface is achieved by minimizing the mean square surface error of the corrected optical surface. The corrected displacement of the ith node, ds_i^{Corr}, is the sum of the uncorrected displacement of the ith node, ds_i, and the displacements induced by each actuator,

$$ds_i^{Corr} = ds_i + \sum_j \mathbf{x}_j dx_{ji}$$

(2.1)

where x_j is the variable actuator input for the jth actuator, and dx_{ji} is the displacement of the ith node for the jth actuator's influence function. The mean square residual error, E, of the corrected optical surface is represented by,

$$E = \sum_i w_i \left(ds_i + \sum_j x_j dx_{ji} \right)^2$$

(2.2)

where w_i is the area weighting of the ith node.

The actuator inputs that minimize the mean square error, E, are found by taking derivatives of Eqn. (2.2) with respect to each actuator input, x_j, and setting each resulting equation equal to zero. This results in the following linear system represented by Eqn. (2.3):

$$[H]\{X\} = \{F\},$$

(2.3)

where

$$H_{jk} = \sum_i w_i dx_{ji} dx_{ki},$$

(2.4)

and

$$F_k = \sum_i w_i ds_i dx_{ki}.$$

(2.5)

The adaptive mirror's residual RMS surface error, $\sqrt{E}$, may be computed with the use of Eqn. (2.2) once the actuator inputs have been found from Eqn. (2.3), (2.4), and (2.5).

2.2   System Level Performance

While it may be useful in some applications to predict the adaptive control performance of a single optical surface, a much more powerful tool is to be able to predict the adaptive performance of an entire optical system as discussed in Section 1. This approach is based upon the method of superposition and the linearity of Zernike polynomials in the wavefront with Zernike polynomials and rigid body motions describing the deformations and motions of optical surfaces.[8] For the small surface perturbations typical of adaptive optical systems, this approximation is generally valid. This computation is performed by importing the changes in the wavefront error of each Zernike polynomial at a location of optical performance measurement (e.g., the focal plane) with respect to changes in the rigid body motion and Zernike polynomials of surface deformation of each optical surface in the system. These sensitivities can be computed in an automated fashion by optical design software. With this matrix of information we are able to compute the performance of the optical system due to any deformations and motions of the optical surfaces as long as they can be described by the rigid body motions and Zernike polynomials used in the development of the optical sensitivity matrix. Notice that the optical sensitivity matrix needs only to be generated once before any mechanical analysis as long as the optical prescription (shape and location of the optical surfaces) does not change. This method of system level optical performance prediction can be extended to adaptive control prediction in a similar method as was used in Section 2.2.

The mathematical description for performing integrated adaptive analysis using Zernike decomposition techniques is provided below. An optical sensitivity matrix, S_{kj}^n, represented by a set of Zernike terms, k, at the location of optical performance measurement, is computed from the optical system analysis model by perturbing each optical surface, n, by a unit surface perturbation, j. Each of the unit surface perturbations is either a rigid body motion or a Zernike polynomial. Enough of these perturbations are chosen to adequately describe the expected deformations of the optical surfaces.

Once the optical sensitivity matrix has been generated, each actuator influence function, Φ_m, where m is the actuator, is decomposed into rigid body motions and Zernike polynomials, B_{jm}, by simple polynomial fitting, where, j is the rigid body motion or Zernike polynomial term fit to the influence function. Notice that both Φ_m and B_{jm} may contain the influence functions from multiple optical surfaces if there is more than one adaptive surface in the system. This polynomial fit is then converted to actuator influence functions of optical performance by,

$$U_{km} = S_{kj} B_{jm}.$$

(2.6)

For a given perturbed state of the optical system due to an environmental load, each deformed surface is similarly decomposed into Zernike coefficients, C_{ji}^n, where, j, is the vector of Zernike coefficients for load case, i, of each optical

surface, n. The wavefront error of the optical system is computed by multiplying the optical sensitivities by the Zernike terms of the deformed surface

$$Z_{ki} = S_{kj}{}^n C_{ji}{}^n \qquad (2.7)$$

where Z_{ki} is vector of Zernike polynomials, k, for each load case, i.

Similar to Eqn. (2.2) fitting the actuators to minimize the optical system wavefront error is performed using a least-squares fit. A system error, E, is defined as

$$E = \sum_k^Z w_k \left(Z_{ki} - \sum_m^M U_{km} A_m \right)^2 , \qquad (2.8)$$

where A_m is the contribution coefficients of each actuator and w_k, is the wavefront RMS error of each polynomial term, k, at the optical performance measurement location.

To compute the best-fit actuator coefficients, the error function is minimized with respect to the actuator contribution coefficients. This is performed by taking the derivative of the error function with respect to these coefficients and setting it equal to zero as follows:

$$\frac{dE}{dA_q} = \sum_k^Z w_k 2 \left(Z_{ki} - \sum_m^M U_{km} A_m \right) U_{kq} = 0 . \qquad (2.9)$$

Rearranging terms yields the following expression:

$$\sum_k^Z w_k \left(\sum_m^M U_{km} U_{kq} A_m \right) = -\sum_k^Z w_k \left(Z_{ki} \right) U_{kq} . \qquad (2.10)$$

The actuator coefficients may be solved via the following matrix equation:

$$[H]\{A\} = \{F\}, \qquad (2.11)$$

where

$$H_{qm} = \sum_k^Z w_k U_{qk} U_{km} , \qquad (2.12)$$

and

$$F_q = -\sum_k^Z w_k Z_k U_{kq} . \qquad (2.13)$$

The adaptive mirror's residual RMS surface error, $\sqrt{E}$, may be computed with the use of Eqn. (2.8) once the actuator inputs have been found from Eqn. (2.11), (2.12), and (2.13).

3   IMPLEMENTATION

A DRESP3 subroutine implementing the methods in Section 2 was used to return the corrected surface RMS error, $\sqrt{E}$, within the design optimization feature of MD Nastran. The subroutine is a modified form of Sigmadyne's commercially available software, *SigFit*. An additional utility was written to write the DRESP3 and other required bulk data. The function of the DRESP3 feature is illustrated in Figure 3. Within the design optimization loop of MD Nastran SOL 200 the Sigmadyne SigFit DRESP3 server is available to provide the optimizer with the adaptively corrected performance of the optical system's current design and local finite difference results used for sensitivity calculations.

3.1   Bulk Data Format

A combination of a DTABLE card and DRESP1 cards were used with the DRESP3 feature.[21] The DTABLE card is used to store the various user selectable option values, prescription data associated with each optical surface, optical surface node locations, and optical surface node area weighting. If the user chooses to perform system level analysis instead of single surface analysis, then the optical surface sensitivity matrix, **S**, is stored on the DTABLE as well. An example DTABLE card is shown in Figure 4.

Figure 3: Flowchart of design optimization with system level optical performance evaluation.

```
DTABLE    ina        1.0 nsym        0.0 nsbc        0.0 ns         3.0
          ngs01    204.0 roc01  -1.015+2 ckk01  -1.00230 ssc01      1.0
          ngs02    145.0 roc02  -1.249+1 ckk02  -1.49690 ssc02      1.0
          ngs03      1.0 roc03       0.0 ckk03       0.0 ssc03      1.0
          irb        0.0 izd        0.0 wvl    3.9370-8 izk         5.0
          nat        9.0 iaa        0.0 ndt        1.0 isys         1.0
          x00001 2.62500 y00001 -1.51554 z00001 -4.520-2 w00001 4.9020-3
          x00002 1.50000 y00002      0.0 z00002 -1.110-2 w00002 4.9020-3
          x00003 2.50000 y00003      0.0 z00003 -3.080-2 w00003 4.9020-3
          .
          .
          .
          x00348 1.20761 y00348 -0.32358 z00348 -6.277-2 w00348 6.8966-3
          x00349 1.44938 y00349 -0.38836 z00349 -9.046-2 w00349 6.8966-3
          x00350      0.0 y00350      0.0 z00350      0.0 w00350  1.00000
          ism01      3.0 nzp01      37.0
          a00001      0.0 a00002      0.0 a00003      0.0 a00004      0.0
          a00005      0.0 a00006      0.0 a00007 -1.135+4 a00008 -1.84-13
          a00009 -5.26-14 a00010 7.079-12 a00011 1.1596+6 a00012      0.0
          a00013 3.715-10 a00014 -1.135+4 a00015 5.8002-7 a00016 -1.160+6
          .
          .
          .
          a00213 -1.389-6 a00214 1.3149-3 a00215 1.3136-3 a00216      0.0
          a00217 3.3925-6 a00218 2.4075-6 a00219 -5.857-6 a00220 -2.017-3
          a00221 -2.016-3 a00222      0.0
          b00001      0.0 b00002      0.0 b00003      0.0 b00004      0.0
          b00005      0.0 b00006      0.0 b00007      0.0 b00008      0.0
          b00009      0.0 b00010      0.0 b00011      0.0 b00012      0.0
          .
          .
          .
          b01361 1.3808-5 b01362 5.8228-5 b01363 5.8227-5 b01364 1.5570-4
          b01365 2.1019-4 b01366 1.1025-3 b01367 1.1025-3 b01368 -5.224-3
          b01369  1.98370
          ism02      3.0 nzp02      37.0
          c00001      0.0 c00002      0.0 c00003      0.0 c00004      0.0
          c00005      0.0 c00006      0.0 c00007 1.0250+4 c00008 -3.58-14
          c00009 -1.17-13 c00010 -2.55-12 c00011 -1.290+5 c00012      0.0
          .
          .
          .
```

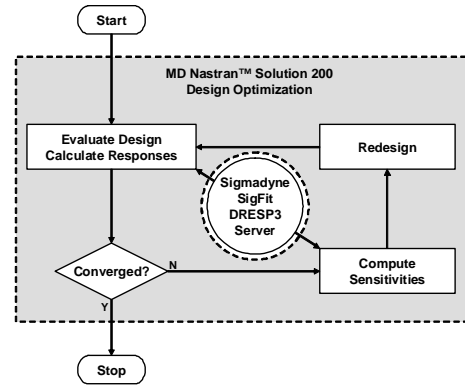**Figure 4:** Example DTABLE card for system level adaptive control analysis.

DRESP1 cards are used to compute the optical surface nodal translations. Nodal rotations are not required. A set of DRESP1 cards covering all optical surface nodes are written for each actuator influence function subcase and disturbance subcase. Example DRESP1 cards are shown in Figure 5.

```
DRESP1    100001D0100001 DISP                                    1           10001
DRESP1    100002D0100002 DISP                                    2           10001
DRESP1    100003D0100003 DISP                                    3           10001
DRESP1    100004D0100004 DISP                                    1           10003
DRESP1    100005D0100005 DISP                                    2           10003
DRESP1    100006D0100006 DISP                                    3           10003
DRESP1    100007D0100007 DISP                                    1           10006
DRESP1    100008D0100008 DISP                                    2           10006
DRESP1    100009D0100009 DISP                                    3           10006
.
.
.
```

Figure 5: Example DRESP1 cards for request of translational displacements of optical surface nodes.

The DRESP3 card is simply written to reference the DTABLE and DRESP1 entries so that they may be exported to the DRESP3 server routine. All of these cards are written by the utility program mentioned above with input from the user.

The DRSPAN card must then be used in case control to assign the sets of DRESP1 cards to their respective subcases as shown in Figure 6.

```
SUBCASE 11
  LABEL=DISPLACEMENT ACTUATOR #1
  LOAD=24101
  SET 11 = 100001 THRU 101050
  DRSPAN=11
SUBCASE 12
  LABEL=DISPLACEMENT ACTUATOR #2
  LOAD=24201
  SET 12 = 200001 THRU 201050
  DRSPAN=12
SUBCASE 13
  LABEL=DISPLACEMENT ACTUATOR #3
  LOAD=24301
  SET 13 = 300001 THRU 301050
  DRSPAN=13
.
.
.
```

Figure 6: Example subcases showing the use of the DRSPAN card.

3.2   Example

An example telescope model is used to demonstrate the optimization of an orbiting telescope's adaptive primary mirror. A plot of the telescope model is shown in Figure 7. The primary mirror is of lightweighted construction composed of a lightweighted triangular cell core with front and back faceplates. A primary mirror reaction structure provides mounting locations for three displacement actuators and six force actuators. This reaction structure also supports the focal plane unit behind the primary mirror. An Invar shell is used to meter a secondary mirror assembly comprised of the secondary mirror and spider structure. Six main struts are used to mount the telescope to the spacecraft bus.
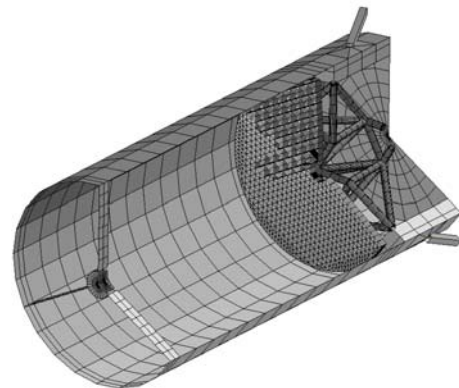

Figure 7: Finite element model of orbiting telescope.

The goal of the optimization is to minimize the weight of the adaptively controlled primary mirror while constraining the optical performance of the telescope as shown in Figure 1. The optical performance is measured by the wavefront error at the exit pupil of the telescope system. Several design variables

relating to the design of the primary mirror are defined. These variables include the depth of the mirror core, the thicknesses of the facesheets, and the wall thicknesses of various regions of the mirror core as shown by the shading in Figure 9. The thickness variables were defined such that thicknesses could be designed near each of the mounts and actuators. Additional requirements were imposed consisting of a minimum natural frequency and a launch stress allowable. The optimization problem is formally defined as follows:

MINIMIZE:
      Weight of primary mirror

DESIGN VARIABLES:
      Optical facesheet thickness: 0.18 inch $< t_f < 0.25$ inch
      Back facesheet thickness: 0.10 inch $< t_b < 0.25$ inch
      Interior core wall thicknesses: 0.04 inch $< t_c < 0.25$ inch
      Inner and outer core wall thicknesses: 0.08 inch $< t_c < 0.25$ inch
      Core depth: 0.25 inch $< t_c < 5.0$ inch

SUBJECT TO:
      Thermally induced system wavefront error < 20 nm RMS
      Gravity release induced system wavefront error < 60 nm RMS
      Peak launch induced stress in PM < 1000 psi
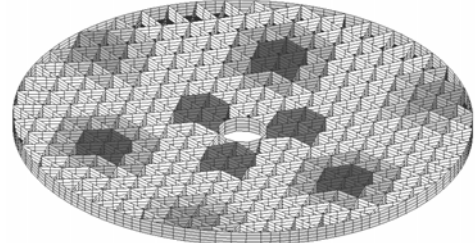   First mounted PM natural frequency > 200 Hz

Figure 8: Core thickness variables shown by shading.

The analysis results for the initial design and the optimized design are shown in Table 1 alongside the requirements. Notice that the optimizer reduces the weight of the primary mirror by over 50% while the constraints on system wavefront error, launch stresses, and natural frequency are obeyed. It is important to notice that the stress constraint is already active in the initial design while the gravity induced wavefront error constraint is nearly active.

Table 1: Results of Design Optimization

Response	Initial Design	Optimized Design	Requirement
Thermally Induced Wavefront Error	9 nm	20 nm	20 nm
Gravity Release Induced Wavefront Error	54 nm	60 nm	60 nm
Peak Launch Stresses	1000 psi	1000 psi	1000 psi
First Natural Frequency	231 Hz	221 Hz	200 Hz
Weight	20.8 kg	9.9 kg	Minimum
Areal Density	53.0 kg/m^2	25.2 kg/m^2	Minimum

Notice that the use of the system level optical performance as a response allows the design of the primary mirror to develop into a design which best corrects the system wavefront error rather than only the wavefront error of the primary mirror assembly. The optimum primary mirror design, therefore, includes the best mix of design characteristics for correcting the errors from the secondary mirror assembly, the errors from the metering structure, as well as the errors from the primary mirror assembly. This approach gives the optimizer more freedom in finding an optimum design compared to the method of Figure 1 which optimizes each subsystem independently to separately allotted requirements.

4   IMPROVEMENTS

4.1   DRESP3 Gradient Calculation

The method used to compute design sensitivities of DRESP3 responses with respect to the design variables prior to V2008R1 was not as efficient as it could be for responses with many DRESP1 arguments. On page 56 of the MSC.Nastran 2004 Design Sensitivity and Optimization User's Guide the equation for an example sensitivity of a DRESP2 or DRESP3 with respect to a design variable is written in Eqn. 2-38. A more general form based on this equation is,

$$\frac{dr}{dX_i} = \sum_{j=1}^{N_a} \frac{\partial r}{\partial a_j}\frac{\partial a_j}{\partial X_i} = \sum_{j=1}^{N_a} \left[\frac{r\left(\mathbf{a}(\mathbf{X^0})+\Delta a_j\right) - r\left(\mathbf{a}(\mathbf{X^0})-\Delta a_j\right)}{2\Delta a_j} \right] \frac{\partial a_j}{\partial X_i} , \qquad (4.1a)$$

$$\frac{\partial a_j}{\partial X_i} = \left[\frac{a_j\left(\mathbf{X^0} + \Delta X_i\right) - a_j\left(\mathbf{X^0} - \Delta X_i\right)}{2\Delta X_i} \right], \tag{4.1b}$$

where, r is the DRESP2 or DRESP3 synthetic response, N_a is the number of arguments sent to the DRESP2 or DRESP3, a_j is the jth such argument of the vector of design variable dependent arguments $\mathbf{a(X^0)}$, X_i is the ith design variable value of the vector of current design variable values, $\mathbf{X^0}$, Δa_j is the finite difference step of the jth argument, and ΔX_i is a finite difference step of the ith design variable. Eqn. 4.1b is required for use with any argument a_j for which a finite difference calculation must be used to compute the gradient with respect to the design variable X_i. This equation has the disadvantage that two evaluations of the synthetic response are required for each argument which has a nonzero sensitivity with respect to a design variable. For the purposes of optical surface evaluation in which there are many nodal displacements involved, this can be very computationally expensive.

A more efficient form for sensitivity computation for response, r, would be,

$$\frac{dr}{dX_i} = \frac{r\left(\mathbf{a(X^0)} + \Delta X_i \frac{\partial \mathbf{a(X^0)}}{\partial X_i}\right) - r\left(\mathbf{a(X^0)} - \Delta X_i \frac{\partial \mathbf{a(X^0)}}{\partial X_i}\right)}{2\Delta X_i} \tag{4.2a}$$

$$\frac{\partial \mathbf{a(X^0)}}{\partial X_i} = \frac{\mathbf{a}\left(\mathbf{X^0} + \Delta X_i\right) - \mathbf{a}\left(\mathbf{X^0} - \Delta X_i\right)}{2\Delta X_i}, \tag{4.2b}$$

where, X_i is the ith design variable value of the vector of current design variable values, $\mathbf{X^0}$, $\mathbf{a(X^0)}$ is the argument list of the DRESP2 or DRESP3 evaluated at the current design variable values, and ΔX_i is a finite difference step of the ith design variable. This method was implemented in V2008R1 when the argument list is comprised of only DTABLE and DRESP1 quantities and when the number of DRESP1 arguments exceeds the number of design variables.[22] This improvement has resulted in the ability to use the DRESP3 for system level adaptive control simulation whereas the prior algorithm rendered the feature unusable.

5   CONCLUSIONS

A method for incorporating multidisciplinary optimization in the design process of optical systems was presented. The process is highlighted by being able to predict the system level optical performance during automated optimization of the mechanical design. The use of this system level performance in design optimization allows the optimizer to find designs which might be unrealizable by independent subsystem optimization. This process would be most effective early in the design process when various system concepts are being compared. This method allows engineer's to quickly obtain a rough estimate of the optimum design for the system. Once this has been done for each concept being considered a final selection of the best concept can be made. The resulting subsystem designs and error allocations found by the optimizer can then be given to separate design teams for more detailed design work to be performed in parallel.

The addition of the DRESP3 to MSC.Nastran SOL 200 is a powerful improvement to the design optimization features. The DRESP3 allows the user dramatically more capability than available before. Such capability allows engineers to make engineering predictions which were never before possible within the bounds of a finite element code.

6   REFERENCES

1. G. Michels, V. Genberg, "Opto-mechanical analysis and design tool for adaptive X-ray optics," SPIE Vol. 7803 (7), San Diego, CA, August, 2010.
2. S. Roberts, "Systems engineering of the Thirty Meter Telescope through integrated opto-mechanical analysis", SPIE Vol. 7738, San Diego, August, 2010.

3. K. Doyle, "Antenna performance predictions of a radio telescope subject to thermal perturbations," SPIE Vol. 7427 (12), San Diego, CA, August, 2009.
4. D. Kerley et. al., "Validation and verification of integrated model simulations of a thirty meter telescope", SPIE Vol. 5867, San Diego, August, 2005.
5. K. Doyle, V. Genberg, G. Michels, G. Bisson, "Optical modeling of finite element surface displacements using commercial software", SPIE Vol. 5867 (18), San Diego, CA, August, 2005.
6. V. Genberg, K. Doyle, G. Michels, "Optical Interface for MSC.Nastran", MSC 2004 VPD Conference, Huntington Beach, CA, October, 2004.
7. V. Genberg, K. Doyle, G. Michels, "Optical performance as a function of dynamic mechanical loading", SPIE Vol. 5178 (4), San Diego, CA, August, 2003.
8. K. Doyle, V. Genberg, G. Michels, "Integrated optomechanical analysis of adaptive optical systems", SPIE Vol. 5178 (5), San Diego, CA, August, 2003.
9. Doyle, Keith B., Victor L. Genberg , Gregory J. Michels, Integrated Optomechanical Analysis, SPIE Press, Bellingham, WA, 2002.
10. V. Genberg, G. Michels, K. Doyle, "Making mechanical FEA results useful in optical design", SPIE Vol. 4769 (4), Seattle, WA, July, 2002.
11. B. Cullimore, T. Panczak, J. Baumann, V. Genberg, M.Kahan, "Integrated Analysis of Thermal/Structural/Optical Systems", ICES Paper, 2002.
12. K. Doyle, V. Genberg, G. Michels, "Numerical methods to compute optical errors due to stress birefringence", SPIE Vol. 4769 (5), Seattle, WA, July, 2002.
13. K. Doyle, J. Hoffman, V. Genberg, G. Michels, "Stress birefringence modeling for lens design and photonics", Invited Paper, International Optical Design Conference, Tucson, AZ, April, 2002.
14. V. Genberg, G. Michels, "Opto-mechanical analysis of segmented/adaptive optics", SPIE Vol. 4444 (10), San Diego, August, 2001.
15. Gregory J. Michels, Victor Genberg, "Design Optimization of Actively Controlled Optics", SPIE Paper 4198 (17), November 2000.
16. A. Williams, V. Genberg, S. Gracewski, B. Stone, "Simultaneous Design Optimization of Optomechanical Systems", SPIE Paper 3786 (28), 1999.
17. V. Genberg, "Optical Performance Criteria in Optimum Structural Design", SPIE Paper 3786 (29), July 1999.
18. A. Williams, V. Genberg, S. Gracewski, B. Stone, "Multidisciplinary Design Optimization of Optomechanical Devices", Proc 3rd WCSMO, 1999.
19. V. Genberg, G. Michels, "Opto-mechanical analysis of segmented/adaptive optics", SPIE Vol. 4444 (10), San Diego, August, 2001
20. K. Doyle, V. Genberg, G. Michels, "Integrated optomechanical analysis of adaptive optical systems", SPIE Vol. 5178 (5), San Diego, CA, August, 2003.
21. Johnson, Erwin H. et al., MSC.Nastran 2004 Design Sensitivity and Optimization User's Guide, MSC.Software, Santa Ana, CA, 2003.
22. MSC Nastran 2008 R1 Release Guide, MSC.Software, June 4, 2008, pp.